

SURFACE STUDIES OF THE INTERACTION OF Cl_2 WITH $\text{InP}(100)(4 \times 2)$; AN INVESTIGATION OF ADSORPTION, THERMAL ETCHING AND ION BEAM ASSISTED PROCESSES

A.J. MURRELL, R.J. PRICE, R.B. JACKMAN and J.S. FOORD

Inorganic Chemistry Laboratory, University of Oxford, South Parks Road, Oxford OX1 3QR, UK

Received 10 July 1989; accepted for publication 29 November 1989

The reactions of chlorine on the $\text{InP}(100)(4 \times 2)$ surface have been investigated using LEED, AES and TDS techniques. Chlorine forms a strongly bound chemisorbed monolayer on the semiconductor surface during low gas exposures. At high gas exposures, bulk corrosion sets in and an In-rich chloride film is formed at the interface which desorbs as InCl_3 . The degree of surface segregation which takes place is found to depend on the chlorine dosing pressures employed and the chemistry exhibited is also very sensitive to the state of the semiconductor surface; on In enriched interfaces corrosion takes place some 300 times more rapidly and InCl rather than InCl_3 is the desorbing product. The surface transformations brought about by low energy ion beams are investigated. Ion beam irradiation sputters InCl and P_4 from the chloride layer and converts the chloride rich corrosion scale into InCl . A mechanism for ion beam assisted etching is proposed and the results compared to previous studies.

1. Introduction

Chemical reactions at the semiconductor-halogen interface have attracted considerable attention, both because of the varied surface chemical phenomena which these systems exhibit and also because of their technological relevance to the dry etching of semiconductor materials [1–13]. The points of interest include the adsorption kinetics of both halogen molecules and atoms, the atomic and electronic structures of the chemisorbed layers and corrosion phases produced, and desorption reactions, which liberate halides and other molecules derived from the semiconductor material. Additionally it is of interest to consider how halogen adsorption and subsequent desorption of reaction products can influence surface stoichiometries in the case of compound semiconductor materials. The desorption reactions, which result in etching of the surface, may be thermally driven or enhanced by irradiation from photon, electron or ion sources [5–13]. This opens up the possibility of non-lithographic patterning and low temperature etching of semiconductor surfaces using focused beams while generating attention in photon and ion induced surface chemistry.

In this paper we have studied the interaction between $\text{InP}(100)$ and chlorine using LEED, AES and thermal desorption measurements as a function of chlorine pressure and surface stoichiometry, and also investigated the effects of low energy ion beams on the reactions observed. Montgomery et al. [2] have examined the adsorption of chlorine on $\text{InP}(110)$ surfaces using Auger electron spectroscopy (AES) and ultraviolet photoelectron spectroscopy (UPS) and found evidence both for a two stage adsorption process and depletion of phosphorus from the surface at high chlorine exposures. Studies of ion beam assisted etching reactions by McNevin [12] have concentrated on product analysis in steady state etching reactions, with limited investigation of the surface before and during ion beam irradiation. Our results will be discussed with reference to this previous work and studies which have been carried out in related systems.

2. Experimental

All experiments were carried out in a stainless-steel ultra-high vacuum chamber, pumped by dif-

fusion pump, in which base pressures of 2×10^{-10} mbar were regularly achieved. The chamber incorporated a four-grid retarding field electron optics for LEED and AES measurements, and a 0–200 a.m.u. quadrupole mass spectrometer for thermal desorption spectroscopy (TDS), residual gas analysis and ion-beam sputtered product analysis. The ion source was a low energy (500 eV, 0.05 A m^{-2}) argon ion gun, which was also used to clean the samples. The samples used (n-type $\text{InP}(100)$) were cleaned by 30 min bombardment followed by annealing at 650 K for 2 h using a procedure which is similar to that described previously [14]. This yielded a (4×2) reconstructed surface as seen in fig. 2a later. The condition of the sample, which was critical to the results obtained, was found to degenerate with repeated experiments in two respects. Firstly the structure of the surface gradually degraded as a result of the etching and TDS experiments, the (4×2) LEED pattern changing to (4×1) and then to a (1×1) . This could often be rectified by further annealing at 650 K to restore the (4×2) reconstruction. Secondly the stoichiometry of the surface varied as a result of experiments as monitored by AES. To keep this constant an In metal evaporation source was incorporated into the chamber as was a PH_3 cracking source to permit phosphorus dosing. The latter consisted of a quartz tube containing a resistively heated tantalum cracking filament [15]. Prolonged annealing at 650 K following In/P dosing restored the clean (4×2) surface with the original stoichiometry permitting accurately reproducible experiments to be performed.

Chlorine dosing on to the surface was achieved by in situ solid state electrolysis of a Cd-doped AgCl pellet, heated to 370 K to promote ionic conduction [16,17]. The anode of the cell was in close proximity to the sample, allowing high gas fluxes at the surface while keeping the background Cl_2 pressure low. The TDS experiments, which were carried out with the sample directly in front of the mass spectrometer, used a linear heating rate of $\sim 20 \text{ K s}^{-1}$. The ion beam sputtering experiments in which the sputtered products were analysed were carried out with the sample at 45° to both the ion gun and mass spectrometer using an Ar ion beam of 500 eV and current density of

0.05 A m^{-2} . AES measurements employed a 2.5 keV defocussed ($< 0.05 \text{ A m}^{-2}$) electron beam and signal intensities as used in this paper refer to peak-to-peak heights measured in derivative spectra. All results recorded were repeated in several experiments to verify the reproducibility of the observations made.

3. Results

3.1. Chlorine adsorption upon $\text{InP}(100)$

Controlled quantities of chlorine were exposed to an atomically cleaned $\text{InP}(4 \times 2)$ sample at 300 K and Auger electron spectra recorded. Electron stimulated desorption was observed and exposure to the e-beam was therefore minimised. Measurement of the time dependence of the Auger signal intensities, assuming the normal exponential decay, showed that the effects of ESD were very small under the conditions of our experiments. Corrections to extrapolate back to zero e-beam exposure were made although the amendments involved ($< 5\%$) do not influence qualitatively the interpretation of the results. A typical spectrum for a surface exposed to chlorine is illustrated in fig. 1A. It shows peaks corresponding to Auger transitions of phosphorous, chlorine and indium atoms. In fig. 1A we also present a plot of the ratio of the Cl:P Auger peak intensities versus chlorine exposure whilst in fig. 1B we plot out the variations in the P:In ratio during Cl adsorption against the corresponding variations in the Cl:In ratio.

The adsorption kinetics of chlorine on this surface can be seen to involve an initial period of rapid uptake up to an exposure of around 10 L with a much slower but finite adsorption rate beyond this point. This behaviour is qualitatively similar to results of Montgomery et al. [2] on $\text{InP}(110)$. They attribute the period of rapid uptake to the completion of one monolayer coverage of chlorine. If this is the case here then a high initial sticking probability is suggested for chlorine adsorption on $\text{InP}(100)$. In fig. 1B the most noticeable trend observed is that the P/In ratio decreases with increasing coverage. However it also can be seen that the P/In ratio decreases

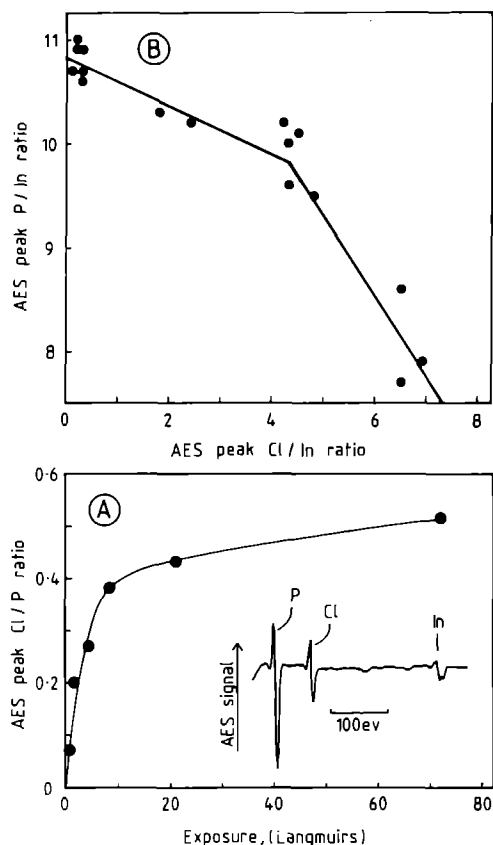


Fig. 1. (A) AES uptake curve for Cl on InP(100) 4×2 at 300 K. Inset: AES spectrum recorded after 60 L exposure. (B) Plot of AES P/In ratio versus Cl/In ratio. Auger signals used: P $L_{2,3}VV$ (120 eV); In $M_{4,4}NN$ (404 eV); Cl $L_{23}M_{23}M_{23}$ (181 eV).

more rapidly at high chlorine coverages than during the initial stages of adsorption. This suggests qualitatively that a change in the nature of adsorption occurs within the exposure regime investigated.

Observations were also made to study the variations in LEED during chlorine adsorption. Fig. 2a shows the (4×2) pattern characteristic of the well ordered clean surface while figs. 2b–2d represent the patterns observed after increasing chlorine exposure. The data reveals that the (4×2) surface reverts to a (4×1) structure at low chlorine coverages which in turn reverts to a (1×1) configuration pattern as more chlorine adsorbs. The intensity of this (1×1) pattern increases with chlorine exposure up to the breakpoint in the graphs presented in fig. 1. However at greater

exposures the diffracted beams all become progressively weaker until they disappear into the background intensity at very high adsorbate coverages corresponding to gas doses of 3000 L or higher.

Further analysis of the chemical nature of these adsorbed phases was performed using TDS. Typical spectra are reproduced in fig. 3. This includes spectra for three species for chlorine exposures up to 3000 L carried out using chlorine surface pressures $< 5 \times 10^6$ mbar. The only fragments observed in the TDS experiment were InCl_x ($x = 0-2$), P_x ($x = 1-4$) and Cl; no Cl_2 or PCl_x species were detected. Fig. 3A shows InCl TDS spectra plotted as a function of Cl exposure. At low coverages a single high temperature peak is observed (570 K), labelled β . For exposures of 50 L and above an additional low temperature peak appears (410 K), labelled α . Fig. 3B shows the corresponding InCl_2 TDS. Here it is apparent that only a low temperature peak is observed. This peak appears initially at the same exposure and follows the same growth kinetics as the α peak in the InCl TDS (fig. 3A). Furthermore the InCl_2 spectra have peak profiles identical to those for the InCl α peak. We therefore conclude that the InCl α peak represents a species formed by ion source fragmentation of a higher chloride and a similar conclusion can also be reached with regard to the In^+ spectra recorded. The desorption spectra for P_4 are shown in fig. 3C; spectra for P_x ($x = 1-3$) were similar and again presumably arise from ion source fragmentation. The spectra reveal a major peak at slightly higher temperatures than the InCl β peak and only a very small low temperature peak indicating very little phosphorus desorbs from the α state.

Fig. 4 shows a plot derived from the spectra in fig. 3A, in which the areas under the two peaks are plotted as a function of exposure. It can be seen that the β state populates rapidly at low exposures but that at higher exposures population of this state slows. The α state only fills at exposures greater than 15 L although the rate at which this occurs is much slower than the initial rate for the β state. It was also observed in these adsorption experiments that the rate at which the α state populated was crucially dependent on the

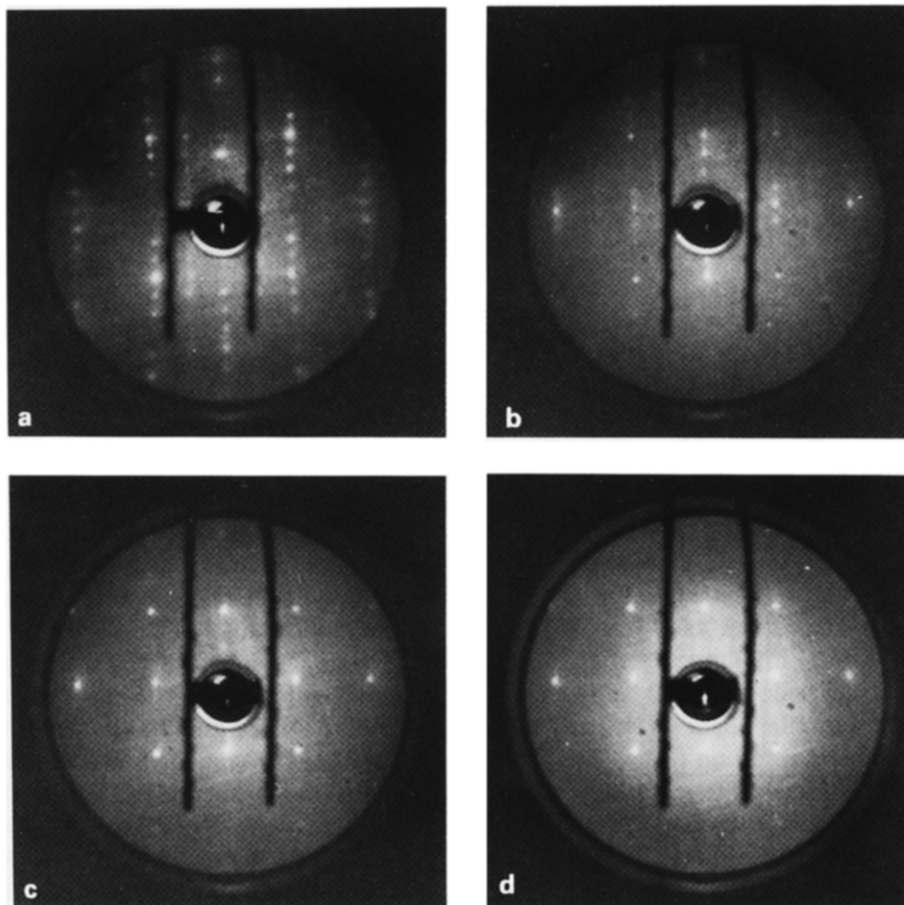


Fig. 2. LEED patterns from $\text{InP}(100)$. (a): clean (4×2) reconstructed surface. (b), (c), (d): after exposure to 2 L, 4 L, 6 L, 10 L, Cl_2 .

stoichiometry and structure of the surface. Reduction in the P/In ratio by evaporation of In on to the surface, or disruption of the surface structure by Ar^+ ion bombardment both resulted in a marked increase in the rate of Cl uptake into the α state. The precise state of the surface therefore markedly influences the adsorption reactions which take place.

Unusually it was also found that the observations depended on the pressures (in addition to the actual gas exposures) at which the chlorine dosing was carried out. The results presented above all employed dosing pressures $< 5 \times 10^{-6}$ mbar. Results shown in fig. 5 illustrate how the TD spectra vary with gas pressure for the same absolute chlorine exposures. At pressures up to 5×10^{-5} mbar the spectra display peaks at tempera-

tures previously assigned to the α and β states. However, above this pressure the α and β peaks disappear to be replaced by a new desorption peak at 600 K which we label γ . The desorption yield increases at these high chlorine pressures and this is also in line with AES measurements which revealed higher Cl/P Auger intensity ratios.

3.2. Chlorine adsorption on $\text{InP}(100)$ with coadsorbed In

As was mentioned in the previous section the results were dependent on the precise state of the InP surface. To investigate this more carefully experiments were carried out in which indium was evaporated on to the surface in order to vary the stoichiometry in a controlled manner. Experi-

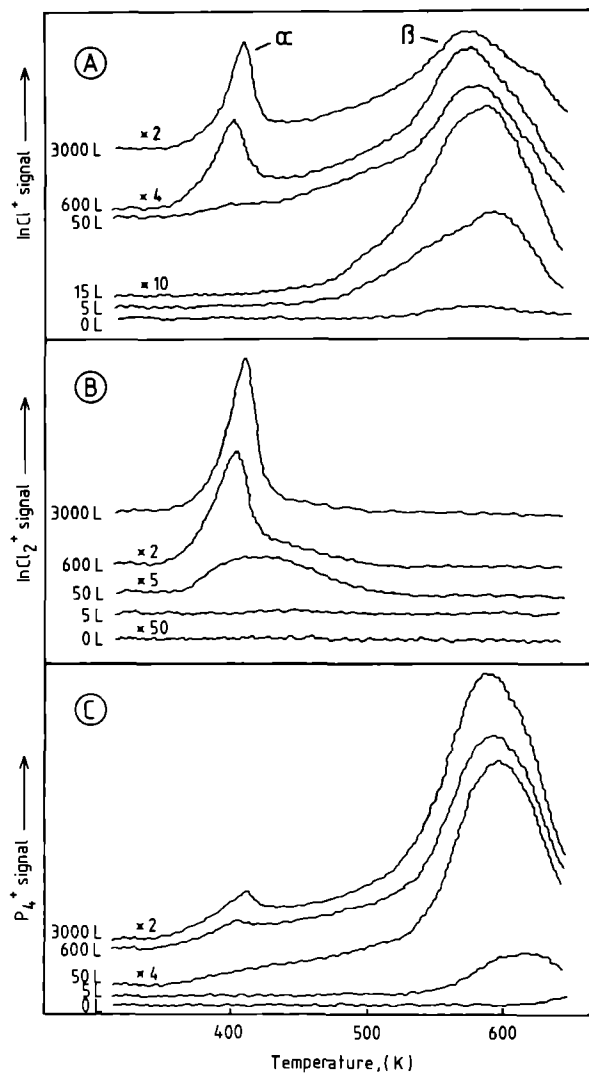


Fig. 3. TDS spectra monitoring. (A) InCl^+ , (B) InCl_2^+ , (C) P_4^+ species following chlorine exposure to $\text{InP}(4 \times 2)$ at 300 K.

ments were performed using a thin layer of indium which resulted in a fall in the P:In Auger intensity ratio from 10 to 4. Fig. 6A shows InCl TD spectra for varying chlorine exposures on this surface. There is a strong resemblance to the corresponding spectra presented previously for surfaces without adsorbed In^+ . However the α peak is shifted from 410 K to 360 K and the β peak from 570 K to 480 K. Also in contrast to the experiments in the previous section no signals

were observed corresponding to InCl_2 or P_x ion currents.

Fig. 6B shows a plot of the areas of the α and β peaks in fig. 6A, as a function of chlorine exposure. This is similar to the corresponding plot for the P rich surface in fig. 4, with the β state initially populating rapidly and the α state populating only at higher exposures as the β state population slows (experiments with gas exposures up to 100 L confirmed that the β state is essentially saturated at 10 L). However there is a very marked difference in the relative rates of initial population of the two states. While the initial β state population rate is comparable for the P rich and In covered surfaces, that of the α state is much more rapid on the In covered surface, the gradient in fig. 6B being a factor of 300 larger than that in fig. 4.

3.3. Ion beam enhanced reactions at the $\text{InP}-\text{Cl}_2$ interface

Experiments were carried out in which adsorbed chlorine layers on the (4×2) InP surface were irradiated with low energy ion beams (500 eV Ar^+). The first experiments were aimed at comparing the sputtered products from clean InP

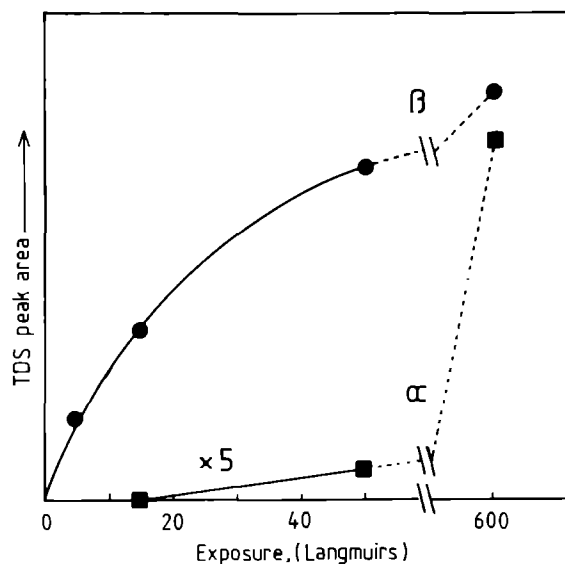


Fig. 4. Uptake curves for the α and β states as derived from InCl^+ thermal desorption yields.

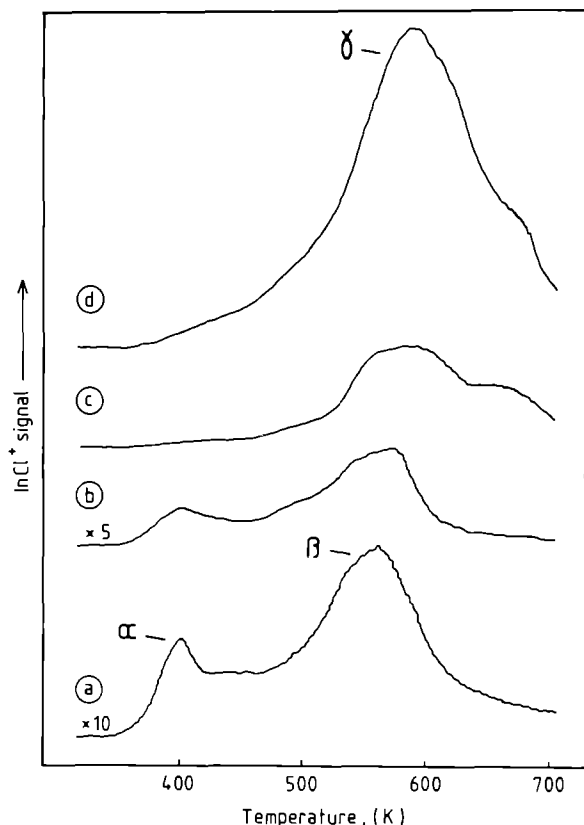


Fig. 5. InCl^+ thermal desorption spectra from $\text{InP}(100) 4 \times 2$ following exposure to 2000 L chlorine at pressures of: (a) 10^{-5} mbar, (b) 5×10^{-5} mbar, (c) 10^{-4} mbar, (d) 2×10^{-3} mbar.

surfaces with interfaces exposed to chlorine. The principle sputtered products from clean InP were In and P_2 ; experiments with the mass spectrometer ion source filament extinguished revealed that approximately half the detected In signal was associated with positive In^+ ions while no P_x ions were detected. The estimated ion source efficiency is 10^{-3} implying that the emitted ions make a negligible contribution to the desorbing flux. A large chlorine exposure prior to irradiation, sufficient to populate both α and β states, resulted in the appearance of P_4 as an additional sputtered product. The associated signal showed an initial rapid rise followed by exponential decay; InCl and Cl (QMS cracking fragment of InCl) signals were also detected which showed a similar behaviour. In and P_2 species were observed with a reduced initial intensity in comparison to the clean

surface signal levels which however increased to these original levels as the P_4 , InCl and Cl signals decayed to zero. The results indicate that Ar^+ ion bombardment of the chlorine covered surface yields predominantly P_4 and InCl species in comparison to In and P_2 which are characteristic of the clean surface.

The InP surface was exposed to 500 L of chlorine and then irradiated with Ar^+ ions for a measured time interval before recording a TD spectra. Fig. 7A shows desorption spectra for the InCl_2 fragment as a function of irradiation time, and reveals a rapid loss of intensity from the α state in the first second. Interestingly, however, over this

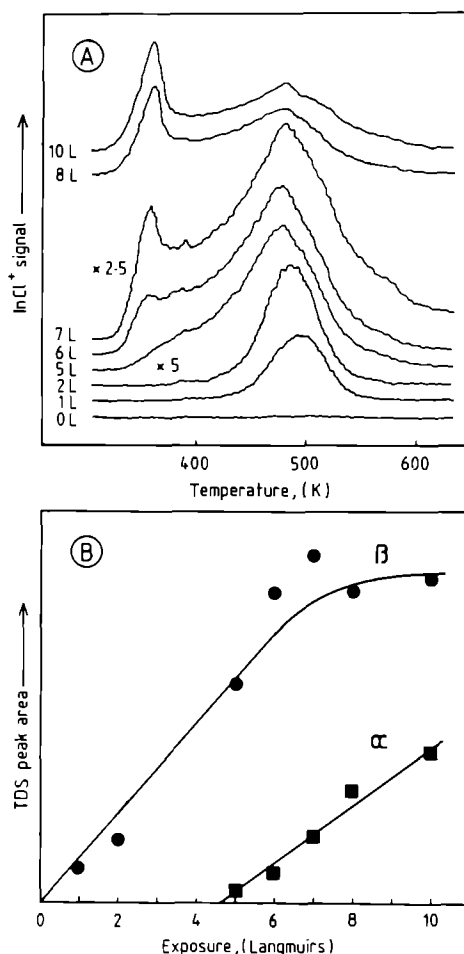


Fig. 6. (A) InCl^+ thermal desorption spectra from the In closed InP surface (see text) following exposure to chlorine. (B) Uptake curves derived from the data in A.

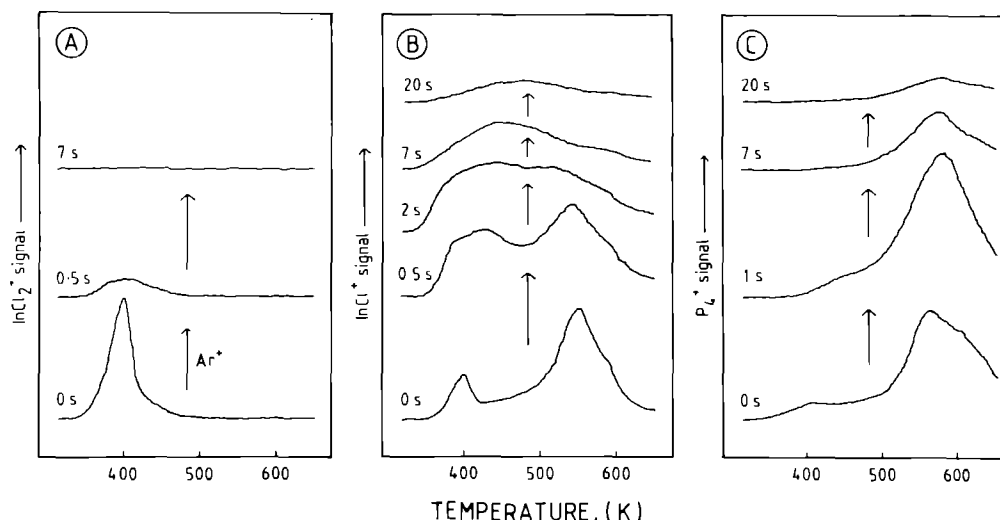


Fig. 7. Thermal desorption spectra from an InP(4 × 2) surface dosed with 500 L chlorine and then Ar⁺ ion bombarded for various times prior to recording the desorption spectrum.

same time scale very little chlorine is lost from the surface as judged by AES. Figs. 7B and 7C show respectively that the desorption yield of InCl and P₄ (as judged by the areas under the curves) both increase in size over this time period. The pronounced structure in the InCl TDS profiles is lost as the irradiation time is increased. Finally the P₄ and InCl desorption yields were found to decay to zero over the 20 s timescale in which AES indicated all the chlorine was sputtered from the surface.

4. Discussion

4.1. Chlorine adsorption upon InP(100)(4×1)

Both the thermal desorption data (fig. 3) and the Auger uptake results (fig. 1) indicate that chlorine adsorption on InP(100) is a two stage process as has been reported for InP(110) [2]. The β state as measured by the thermal desorption yield is populated rapidly in the first stage up to a saturation coverage. Subsequently the α state is seen to populate more slowly without a limiting coverage being detected in the exposure regimes investigated in this work. This shows that the β phase is associated with a 2D chemisorbed adlayer

while the α phase arises from the growth of a bulk corrosion phase. Similar observations have been reported previously for halogen adsorption both on Si [1] and transition metals [19,20].

It is apparent from the exposure needed to populate the β state that the initial sticking probability of chlorine on InP(100) must be close to unity. The thermal desorption data unambiguously shows that the chemisorbed phase dissociates prior to desorption since no Cl₂ is evolved as the layer is thermally decomposed; the layer is likely to be dissociated at room temperature also if it follows the behaviour seen in other halogen chemisorption systems (e.g. refs. [1,19,20]). The LEED results reveal that chlorine chemisorption lifts the surface reconstructions characteristic of the clean surface while the intensities of the (1 × 1) diffracted beams reach a maximum at saturation of the β state suggesting that chlorine forms an ordered (1 × 1) array. During formation of this adlayer the P:In Auger intensity ratio decreases by approximately 10% which is easily accounted for on escape depth arguments bearing in mind the very differing kinetic energies of the In (404 eV) and P (120 eV) Auger electrons monitored. The implication is that the P:In surface stoichiometry does not change markedly during formation of the chemisorbed layer. The (4 × 2) surface is In

terminated [14] and so the adsorbed chlorine must be bonded to these surface In species. However it has been reported [14] that the outer InP(4×2) is incomplete and the formation of a (1×1) In–Cl adlayer would therefore require some In enrichment of the outer layer. The failure to detect this in AES must arise either from the lack of surface sensitivity of this technique or from the presence of defects comprising In vacancies to which LEED is insensitive.

The desorption of this layer in the form of InCl is in line with the structure discussed above. Desorption of InCl over Cl is expected on energetic grounds if the activation energy for InCl desorption is less than that for Cl evolution. If we equate activation energies with heats of reaction (as is often done for desorption processes) then we can show that the difference in desorption activation energies is given by:

$$E_{\text{Cl}}^* - E_{\text{InCl}}^* = D_{\text{InCl}} - E_{\text{In}},$$

where:

E_X^* = desorption activation energy of species X,

E_{In} = desorption energy of In from InP at the In vacancy site created by desorption of InCl,

D_{InCl} = gas phase bond dissociation energy of InCl.

Thermodynamic data on the heat of formation of InP and the heats of atomisation of indium and phosphorus [21,22] indicate that the In–P bond strength in InP is 262 kJ mol⁻¹, thus E_{In} is 524 kJ mol⁻¹ if the desorption energy of In simply involves the cleavage of the two backbonds in the bulk terminated crystal. D_{InCl} is 440 kJ mol⁻¹ hence desorption of Cl rather than InCl should occur which is not observed. The discrepancy could arise in two ways: (i) InCl desorption dominates because of a more favourable entropy of activation. (ii) E_{In} is less than the value estimated, which would be the case for example if the backbonds to surface In were weaker than to surface P, or if desorption occurs from high energy defect sites where the In is much more weakly bound.

A complete adsorption–desorption cycle involving monolayer chlorine adsorption at 300 K and subsequent heating up to 650 K left the

InP(100)(4×2) surface unchanged as judged by LEED and AES. It is apparent from the results discussed above that Cl selectively removes In in the form of volatile InCl. It thus follows that elemental phosphorus must also be lost from the surface during the cycle and this therefore explains the P₄ peak seen in the desorption spectrum at marginally higher temperatures than the InCl peak. Chlorine removes In from the surface to produce a phosphorus rich interface which is unstable under UHV at high temperatures and the interface thus decomposes evolving phosphorus to revert back to the In-rich (4×2) reconstruction.

Above exposures of 10 L bulk corrosion is observed to occur. The adsorption rate data as derived from thermal desorption (total yield) and Auger (area average) uptake curves demonstrate that this process occurs approximately three hundred times more slowly than formation of the adsorbed layer. The P:In Auger ratio starts to drop dramatically when corrosion sets in suggesting that phosphorus is significantly depleted in comparison to In in the growing corrosion phase, although the influence of changes in chemical state on the PL_{2,3}VV transition should be borne in mind. However the thermal desorption data (fig. 3) reveal that virtually no phosphorus is evolved in the α state and this therefore confirms that phosphorus depletion occurs. This could arise through the removal of phosphorus from the surface into the gas phase in the form of volatile halides during gas dosing. Alternatively segregation by diffusion could take place with phosphorus enrichment of the near surface region below the corrosion layer. No phosphorus chlorides were detectable in QMS during chlorine adsorption and repeated adsorption–desorption cycles involving growth–desorption of the α state resulted in a pronounced phosphorus enrichment of the surface as judged by AES. The second suggested explanation is therefore operative in this system. The enhancement of the group V element concentration in the surface layers which halogen adsorption–desorption cycles induce on InP is similar to the results reported for InSb [3].

While our QMS could not monitor InCl₃, the similarity of the relative InCl₂, InCl and In signal intensities to the cracking pattern for the trichlo-

ride show this is the main α state desorption product since the cracking pattern for InCl₂ is quite different [12]. The α peak exhibits fractional order desorption kinetics which appears to be general to the growth of halogen corrosion layers [1,19,20]. Although the desorbing species is thought to be InCl₃, the stoichiometry of the adsorbed phase could differ from this. No In enrichment of the surface was seen after thermal desorption of thick corrosion films but the activation energy for desorption (108 kJ mol⁻¹) of the α peak as deduced from Arrhenius plots of leading edges of the desorption traces is substantially smaller than the heat of sublimation of InCl₃ (157 kJ mol⁻¹). This suggests that the stoichiometry of the corrosion layer must be close to that of the trichloride but the stability of the surface phase differs from the bulk form of this compound.

Experiments under high vacuum do not normally reveal pressure dependent desorption yields and profiles as indicated by the spectra illustrated in fig. 5. This must arise from a kinetic effect since the surface phases are equilibrated under UHV prior to recording the desorption sweeps, irrespective of dosing pressure. The desorption of the indium chloride(s) is coincident with P₄ at high dosing pressures suggesting a mixed In–P–Cl phase is formed, in marked contrast to the case for low dosing pressures. We propose therefore that the difference arises from a competition between the rate of reaction of the interface with chlorine and the rate of segregation of In and P by diffusion. At low Cl₂ pressures the latter is rapid relative to the former hence pronounced segregation with enrichment of the surface phase by In can occur. At high Cl₂ pressures the situation is reversed and hence no surface enrichment can take place.

4.2. Chlorine adsorption on InP(100)(4×2) enriched with In

Thermal desorption spectra recorded immediately following ion bombardment and annealing of the sample differed from those subsequently recorded in that they exhibited an extra peak at around 500 K and enhanced uptake into the α state. The experiments carried out in which

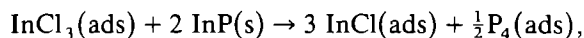
a thin (~ 1 monolayer) In film was dosed onto the surface prior to chlorine exposure show that this is due to enrichment of the surface by In. These enriched In surfaces differ in reaction properties in three respects with regard to the data discussed in the previous section: (i) the desorption temperatures of both states are lower indicative of reduced binding energies. (ii) InCl is the only desorbing species. No InCl₂ or P₄ ion currents are detected. (iii) the rate of uptake into the α state is enhanced. The absence of P₄ desorption demonstrates that the chlorine reacts only with elemental In and does not etch In out of InP. The observations that the reduced desorption energy of the α state (108 kJ mol⁻¹) is now close to the sublimation energy of InCl (111 kJ mol⁻¹) and the desorption product is InCl suggest that the monochloride is the corrosion phase formed in these experiments on the In rich surface. The enhanced rate of uptake is indicative of a more rapid interdiffusion between the corrosion phase and the underlying In than was the case for InP. The standard enthalpy of reaction of indium trichloride with In to form the monochloride is -5 kJ mol⁻¹, while the value for reduction by InP is +52 kJ mol⁻¹ [22]. The observation that the monochloride forms on the In rich surface while the trichloride grows on the InP surface is therefore in line with the thermodynamic properties of the materials concerned.

4.3. Ion beam induced processes

Our results show that the sputtered products from InP change from In and P₂ to InCl and P₄ when the clean surface is reacted with chlorine. The surface concentration of chlorine for interfaces with monolayer coverage as deduced by AES and thermal desorption yields decays with an approximate half life of 10 s in an 500 eV Ar⁺ ion beam of current density 0.05 A m⁻². This indicates that sputtering occurs at a similar rate as on InP itself which is reported to be 0.033 nm s⁻¹ in a similar ion beam [23].

A second point to note is that the ion beam chemically modifies the surface as deduced by the subsequent thermal desorption characteristics. The most rapid change observed is that the InCl₃

desorption signal disappears very rapidly upon irradiation in the ion beam while the InCl and P₄ signals increase. This implies a reaction of the form:



where the phase designation (ads) refers to a phase which desorbs as the species specified. The reaction occurs much more rapidly than the sputtering process since it is essentially completed before any chlorine is lost from the surface. In the presence of Ar⁺ ions, ion beam mixing of the surface layers with the underlying substrate apparently takes place and the kinetic and thermal barriers to monochloride formation are overcome. The thermal desorption characteristics of the InCl(ads) are also modified by ion bombardment as shown by the altered peak profiles with the observed desorption temperature indicating formation of species with binding energies intermediate to those of the α and β states.

The implications of this work for ion beam etching are discussed in section 5.2.

5. Comparison with previous studies

5.1. Thermal processes

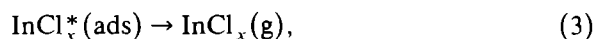
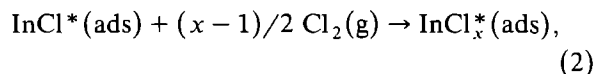
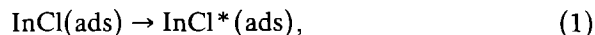
Previous surface science studies on the Cl₂/InP system have been limited to the (110) cleavage plane [2]. The main conclusions to emerge were that chlorine exists on the surface in two distinct forms with P depletion in the outermost layers occurring at high Cl coverages; it was assumed that the two chlorine states could be attributed to molecular and dissociative states. The (100) surface appears to behave similarly to the (110) plane with a two-stage reaction being exhibited and P depletion taking place during the second stage. However we show that the two chlorine states are associated with overlayer formation and bulk compound growth and it seems likely that a similar explanation applies to the (110) surface also. In this respect the InP/Cl₂ system behaves in a similar fashion to other halogen chemisorption systems [1,19,20].

McNevin [12] has studied the steady state thermal etching of InP by chlorine and observes the etch rate becomes negligible below 430 K while the Cl:In and P:In AES intensities change in an abrupt manner at this point. Our work provides an experimental verification that these changes are associated with the bulk halide corrosion phase which desorbs from the surface at approximately this temperature as InCl₃; etching below this temperature is not possible since desorption of etch products is too slow and a passivating scale simply builds up on the surface. McNevin also reports that the etch products are InCl, InCl₂ and P₄. Our studies would predict that the etch products should be P₄ and InCl in the high temperature limit where the Cl coverage is small, with InCl₃ being detected just above the onset temperature. The failure to detect InCl₃ is unsurprising since it will only be observed over a narrow range of steady state conditions. Furthermore the system will tend to move out of this range with positive feedback in view of the fractional order desorption kinetics seen for the α state which implies a desorption energy which increases with coverage. The observation of InCl₂ implies this arises from a transitory surface species which does not possess the surface lifetime required to observe it using the techniques employed in this work.

5.2. Ion beam assisted etching

An energetic Ar⁺ ion striking the substrate surface loses energy in a collision cascade in which the majority of the energy is dissipated by displacing atoms from their initial sites in the solid with additional energy being lost in the form of vibrational and electronic excitations (e.g. ref. [7]). Species can be emitted from the surface during the collision cascade or subsequently desorbed by the "thermal spike" induced by the impinging ion. The enhancement of the thermal etch rate by ion bombardment which may be far beyond that expected for physical sputtering can arise directly from stimulated particle emission or indirectly by promotion of adsorption reactions or surface chemical processes. We observe that the chloride layers formed on InP are only removed rather slowly in the ion beam. The fast ion beam assisted

etch rates which are observed must therefore arise from ion assisted adsorption and surface reaction with impinging chlorine which was not present in our experiments during ion beam irradiation. A reaction scheme of the form



would be consistent with our experimental observations. Our results indicate that the chloride film on InP is rapidly converted in the ion beam to a layer which desorbs as InCl and which is unreactive to further chlorine adsorption; particle emission from this layer is rather slow. Reaction 1 therefore refers to the ion beam induced excitation of the InCl film into a reactive state. Reaction 2 then describes the interaction of this activated surface with the gas phase to form a new surface species which does exhibit fast desorption rates under the etching conditions employed. Reaction 3 refers to the emission of this species, which could occur spontaneously or be stimulated by a second ion. McNevin has reported that InCl₂ increases selectively over InCl during etching in the presence of the ion beam which suggests that $x = 2$ in eq. (2).

P₄ is the observed phosphorus reaction product in both our thermal and ion beam desorption experiments as well as the corresponding steady state etching processes reported by McNevin. Thus apparently chlorine selectively reacts with In and P is simply left to recombine and desorb to restore the surface stoichiometry to within the stable limits. Very little ion beam assisted etching is reported below 430 K, the point at which the bulk corrosion phase desorbs from the surface. The rapid ion beam mixing we observe for very thin corrosion films is presumably ineffective when the thickness of the chloride scale builds up. Hence InCl cannot be rapidly formed and reactions (1) to (3) above do not occur. Finally it is worth

noting that the mechanism for ion beam assisted etching proposed here for InP is rather similar to mechanisms described for the ion beam assisted chlorine etching of both GaAs and Si [4,6], suggesting that the process in these differing systems follows the same pathway.

References

- [1] R.B. Jackman, H. Ebert and J.S. Foord, *Surf. Sci.* 176 (1983).
- [2] V. Montgomery, R.H. Williams and R.R. Varma, *J. Phys. C* 11 (1978) 1989.
- [3] R.G. Jones, N.K. Singh and C.F. McConville, *Surf. Sci.* 208 (1989) L34.
- [4] M. Balooch, D.R. Orlander and W.J. Siekhaus, *J. Vac. Sci. Technol. B* 4 (1986) 794.
- [5] W.L. O'Brien, C.M. Paulsen-Boaz, T.N. Rhodin and L.C. Rathbun, *J. Appl. Phys.* 64 (1988) 6523.
- [6] M.S. Ameen and T.M. Mayer, *J. Appl. Phys.* 63 (1988) 1152.
- [7] J. Dieleman, F.H.M. Sanders, A.W. Kofschoten, P.C. Zalon, A.E. de Vries and A. Honing, *J. Vac. Sci. Technol. B* 3 (1985) 1384.
- [8] R.A. Rossen and H.H. Sawin, *J. Vac. Sci. Technol. A* 5 (1987) 1595.
- [9] F.A. Houle, *J. Chem. Phys.* 79 (1983) 4237.
- [10] F.A. Houle, *J. Chem. Phys.* 20 (1984) 4851.
- [11] H.F. Winters, *J. Vac. Sci. Technol. A* 3 (1985) 700.
- [12] S.C. McNevin, *J. Vac. Sci. Technol. B* 4 (1986) 1203.
- [13] R.M. Osgood, Jr., *Ann. Rev. Phys. Chem.* 34 (1983) 77.
- [14] X. Hou, G. Dong, X. Ding and X. Wang, *J. Phys. C* 20 (1987) L121.
- [15] R. Chow and Y.G. Choi, *J. Vac. Sci. Technol. A* 1 (1983) 49.
- [16] P.J. Goddard and R.M. Lambert, *Surf. Sci.* 67 (1977) 180.
- [17] N.D. Spencer, P.J. Goddard, P.W. Davies, M. Kitson and R.M. Lambert, *J. Vac. Sci. Technol. A* 1 (1983) 1554.
- [18] A.J. Murrell and J.S. Foord, in preparation.
- [19] J.S. Foord and R.M. Lambert, *Surf. Sci.* 115 (1982) 141.
- [20] A.P.C. Reed, J.S. Foord and R.M. Lambert, *Surf. Sci.* 134 (1983) 689.
- [21] R.C. Weast, Ed., *Handbook of Chemistry and Physics* (CRC Press, Boca Raton, 1981).
- [22] S.C. McNevin, *J. Vac. Sci. Technol. B* 4 (1986) 1216.
- [23] N.L. De Meo, J.P. Donnelly, F.J. O'Donnell, M.W. Geis and K.J. O'Connor, *Nucl. Instrum. Methods B* 7/8 (1985) 814.